Chin. Sci. Bull. (2014) 59(36):5227–5234
DOI 10.1007/s11434-014-0619-5

csb.scichina.com
www.springer.com/scp

Review

Condensed Matter Physics

Ammonia borane at high pressures

Jiuhua Chen · Vadym Drozd · Yongzhou Sun · Shah Najiba

Received: 29 April 2014 / Accepted: 20 June 2014 / Published online: 17 September 2014

Abstract Ammonia borane has received tremendous research attention in the past decade because of its potential for chemical hydrogen storage. This paper reviews recent studies about the behavior of ammonia borane at high pressures. While much work is still needed to comprehensively understand the pressure influence on this molecular crystal, a phase diagram based on the available experimental and theoretical data is constructed. Raman spectroscopy studies indicate five transitions upon compression up to 65 GPa at ambient temperature. Diffraction experiments and theoretical studies demonstrate that three of these transitions are first-order phase transformations in the sequence of $I4mm$-$Cmc2_1$-$P2_1$-(different) $P2_1$, and two are iso-structural. A low-temperature phase ($Pmn2_1$) and a high-temperature high-pressure phase ($Pmna$) are also recognized.

Keywords Ammonia borane · High pressure · Raman spectroscopy · X-ray diffraction · Phase transition

SPECIAL TOPIC: High Pressure Physics

J. Chen (✉)
Center for High Pressure Science and Technology Advanced Research, Jilin University, Changchun 13016, China
e-mail: chenjh@hpstar.ac.cn

J. Chen · V. Drozd · Y. Sun · S. Najiba
Center for the Study of Matter at Extreme Conditions, Department of Mechanical and Materials Engineering, Florida International University, Miami, FL 33199, USA

1 Introduction

Although ammonia borane (NH_3BH_3) was first synthesized more than half century ago by Shore and Parry [1], it did not receive dramatic attention until the last decade when it was proposed to be a potential hydrogen storage material [2, 3]. Because of its high hydrogen density, ammonia borane has been extensively studied with regard to its properties related to hydrogen storage since then [4–11]. If taking the lower value of estimated specific energy for hydrogen, i.e., 120 MJ/kg [12], and counting all hydrogen in its formula, ammonia borane has an energy density 6.6 kW h/kg or 3.1 kW h/L. These values are much higher than the ultimate technical performance targets of US Department of Energy for onboard hydrogen storage systems, i.e., gravimetric capacity (2.5 kW h/kg) and volumetric capacity (2.3 kW h/L) for light-duty vehicles [13]. Although these values fall far below the targets when taking other requirements such as delivery temperature and discharge rate into account, ammonia borane is still on the top candidate in chemical hydrogen storage materials.

The details of mechanism for releasing hydrogen from ammonia borane have not been completely comprehended so far. What is well understood is that ammonia borane released hydrogen in three exothermic steps [2, 8, 14–20]. The first step yields hydrogen plus polyiminoborane (PAB: $(NH_2BH_2)_n$), then PAB decomposes to hydrogen plus polyiminoborane (PIB: $(HNBH)_n$) and finally PIB decomposes to hydrogen plus BN. Both experimental and theoretical work [21–23] indicate that the first dehydrogenation process involves the formation of an intermediate, diammoniate of diborane (DADB) complex $[NH_3BH_2NH_3] + [BH_4]$, to overcome the energy barrier for the reaction. Over the past decade, tremendous efforts have gone into improvement to lower the onset temperature of hydrogen release and to increase the kinetics the thermal

decomposition process of ammonia borane. Many approaches such as metal catalysis, Rh [24], Ir [25, 26], In [27–30], Ru [31, 32], Lewis- and Brønsted acid-catalyzed dehydrocoupling [33–35], nano confinement [36–45], additive [46–50] and ionic liquid [51] were tested to solve the problems. Derivatives of ammonia borane by substituting one hydrogen atom of ammonia borane with alkali metal, MNH_2BH_3 (alkali metal amidoboranes), were also reported for improving the dehydrogenation process [52].

High-pressure study of ammonia borane started after the material was recognized for its high potential for hydrogen storage about a decade ago [53, 54]. Applying pressure to this molecular crystal with weak intermolecular interactions introduces a range of changes in atomic bonding and in turn produces crystal structure transitions. Earlier studies were limited to Raman spectroscopy with controversial observations [53, 54] on the pressure where possible new phases appear. The study was soon expanded beyond Raman spectroscopy [55–60] to X-ray/neutron diffraction (XRD/ND) [59, 61–65], infrared (IR) spectroscopy [57], differential scanning calorimetry [66], thermal conductivity [59] and theoretical modeling [61, 62, 64, 67, 68]. A number of pressure-induced phase transitions have been observed in the spectroscopy, diffraction and thermal conductivity experiments. Observations in spectroscopy experiments have a wide range of controversies while diffraction results have a better consistency. Dehydrogenation of ammonia borane at high pressures was investigated using Raman spectroscopy and differential scanning calorimetry. In this paper, we summarize the behavior of ammonia borane, including phase equilibria and crystal structures at high pressures based on the results from these studies.

2 Pressure-induced transitions

2.1 Phase transition from I to III

Ammonia borane experiences a number of phase transformations upon compression. Raman spectra of ammonia borane exhibit five notable changes in the pressure range up to 65 GPa at room temperature (Fig. 1). The first pressure-induced transition from phase I to phase III was observed at a pressure around 1 GPa by Trudel and Gilson [54] and Custelcean and Dreger [53] in 2003 in a diamond anvil cell (DAC). Trudel and Gilson [54] initially reported this transition as two at 0.5 and 1.4 GPa, respectively, based on changes in the slopes of pressure dependence, dv/dP, and splitting of Raman peaks. But the later study by Custelcean and Dreger [53] attributed these changes to one single phase transition and the split of transition pressure in the earlier study to the non-hydrostatic pressure

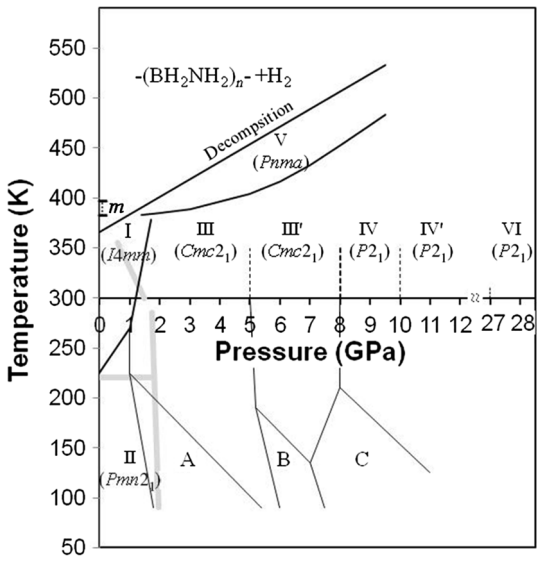

Fig. 1 Summarized *P–T* phase diagram of ammonia borane. I–VI indicated six distinct crystal structures. Phases III and III′, IV and IV′ were iso-structure phases, respectively. Broken lines indicated the boundaries estimated or extrapolated from room temperature and low-temperature data. Gray lines represented the published data that were not adopted in this phase diagram. ***m*** indicated the temperature range of melting when fast heating rates were applied

environment. Custelcean and Dreger [53] used mineral oil as pressure-transmitting medium in the sample chamber of the DAC, whereas no pressure medium was used in Trudel and Gilson's [54] experiment. Further studies [59, 60] confirmed that this phase transition was indeed very sluggish and the two phases may coexist over a wide pressure range (from 0.5 to 2.5 GPa).

The I–III phase boundary has been studied for both high-temperature and low-temperature regions. Chen et al. [63] reported a negative Clapeyron slope of the phase boundary above room temperature in their earlier XRD study in a multi-anvil apparatus, but their later Raman spectroscopy study using a DAC indicates that the boundary has a positive slope [69] and their previous XRD data were likely contaminated by the surrounding sample chamber materials in the solid pressure medium cell assembly. The positive Clapeyron slope above room temperature is consistent with the extrapolation from the II–III phase boundary below room temperature determined by Andersson et al. [59] using in situ thermal conductivity measurements.

2.2 Phase transitions from III to III′, IV and IV′

Lin et al. [55] extended the experimental pressure of Raman spectroscopy study on ammonia to 22 GPa in 2008 using a DAC and observed two additional phase transitions at about 5 and 12 GPa. Based on the features of

characteristic internal modes and the observation of lattice modes, they proposed that the crystal structure of ammonia borane may remain unchanged in the pressure range studied. Xie et al. [57] reported a series transitions in their Raman and IR spectroscopy study at 2.4, 5.5, 8.5 and 10.4 GPa using a DAC. They argued that these transitions are characterized by distinctive profiles and pressure dependences of major modes suggesting possible modifications to the crystal structure of ammonia borane. Because of the sluggishness of the phase I–III transition and the similarity in Raman spectra, the transition at 2.4 GPa from Xie et al.'s [57] experiments could be attributed to the I–III phase transition. The discrepancy in the transition pressure is likely due to the pressure gradient in the DAC sample chamber as no pressure medium was used in both of these experiments and the difference in accuracy of Raman spectroscopy. For the same reason, the transitions observed at 5 GPa by Lin et al. [55] and at 5.5 GPa by Xie et al. [57] are corresponding to the same III–III′ transition, and so are the transitions at 12 GPa by Lin et al. [55] and at 10.4 GPa by Xie et al. [57] corresponding to IV–IV′ transition (Fig. 1). In addition to those transitions observed by Lin et al. [55], Xie et al. [57] recognized a new transition at 8.5 GPa. Because of the feature of continuation weakening and broadening of Raman and IR modes across the boundary at 10.4 GPa, the phase between 8.5 and 10.4 GPa is proposed to be an intermediate phase from ordering to disordering phase at 10.4 GPa. A recent study by Kupenko et al. [70] further extended the experimental pressure of Raman spectroscopy study on ammonia to a much higher pressure (65 GPa) using a DAC and observed another phase transition at 27 GPa.

Filinchuk et al. [61] conducted XRD experiment using a DAC and ab initio calculation in 2009. They demonstrated that the I–III transition at 1 GPa was a first-order structural phase transformation from a disordered phase to an ordered phase. The XRD study by Chen et al. [63] in 2010 indicated that the III–III′ transition at 5 GPa was indeed a second-order iso-structural phase transformation with a discontinuity in their compressibility. The high-pressure phase was much less compressible than the low-pressure phase. Combining density function theory (DFT) calculation and in situ DAC XRD, Kumar et al. [62] demonstrated a structural phase transformation at about 8 GPa and no further structural change up to 27 GPa indicating the III′–IV transition to be a first-order structural transformation and the IV–IV′ transition to be iso-structural.

2.3 Phase transitions at low temperatures

The first report of temperature-induced phase I to II transition at ambient pressure was dated back to 1956 by Lippert et al. [71] and Hughes [72] soon after ammonia borane was discovered. The transition was observed at (230 ± 5) K. However, there was no any further study on the low-temperature transformation at high pressures for more than five decades after this observation. Reynhardt and Hoon [73] revisited this phase transition and refined the transition temperature to 225 K in their nuclear magnetic resonance (NMR) experiment. Raman spectroscopy study by Hess et al. [74] suggested an intermediate phase 10–12 K below the transition. However, this phase has not been confirmed by any other experiments including fine temperature-step neutron diffraction by Filinchuk et al. [61]. Pressure influence on this transition started being investigated only very recently [58–60, 75]. Andersson et al. [59] investigated the pressure dependence of the transition temperature through thermal conductivity experiments using a piston-cylinder high-pressure apparatus as well as Raman spectroscopy and XRD using a DAC in 2011. Their experiments indicated a positive slope for both of the I–II phase boundary and the I–III phase boundary in low-temperature region. Liu and Song [58] also in 2011 suggested that the temperature for the I–II phase transition was nearly independent to pressure (with a slope of 0) and the pressure for the I–III phase transition was independent to pressure (gray lines in Fig. 1) from their Raman spectroscopy experiments. But their phase boundaries were loosely constrained by their experimental data. Their data actually agreed with positive slopes for these transformations as well. A later Raman spectroscopy study by Najiba et al. [75] in 2012 confirmed the positive slope for the I–II phase transition.

Very recently, Najiba et al. [60] extended the pressure range of low-temperature Raman spectroscopy study of ammonia borane to over 10 GPa using a DAC. In addition to I–II and I–III phase boundaries, they determined the boundary between phase II and III with a negative Clapeyron slope. They also determined III–III′ and III′–IV phase boundary in low-temperature region. Both of the boundaries are nearly vertical down to the temperature about 200 K. Below that temperature, three new phases were observed (A, B and C in Fig. 1) in the pressure range up to 10 GPa. Further X-ray/neutron diffraction experiments are needed to clarify the nature of these low-temperature and high-pressure phases.

2.4 *P–T* phase diagram

Ammonia borane has drawn great attentions of research in the past decade, but understanding of its high-pressure behavior is far from comprehensive. Although much work is still needed to complete the *P–T* phase diagram of ammonia borane, an illustrative phase diagram is constructed based on the available data as shown in Fig. 1.

Phase notations are based on the chronological order of the reports for those phases. Phases with alphabetic notations have not yet been confirmed by XRD or ND for their crystal structures. Transitions of phase I to II, I to III, III to IV and those to V were first-order structural phase transformations. Transitions of phase III to III′, IV to IV′ are indentified as iso-structural [62, 63]. The transition from phase IV to VI was observed by Raman spectroscopy study [70] and predicted to be first-order transformation by theoretical study [67]. The boundaries for decomposition and high-temperature phase V were based on Nylén et al.'s [56, 65] Raman spectroscopy and XRD studies; the I–III boundary above room temperature was from Sun et al.'s [69] Raman spectroscopy study; I–II and I–III boundaries below room temperature were from Andersson et al. [59] and Najiba et al. [75]. Other phase boundaries below room temperature were from Najiba et al. [60]; broken lines indicated the boundaries estimated or extrapolated from room temperature data [55, 57] and low-temperature data. Transition at 27 GPa is from room temperature experiment only [70]. Gray lines represent the other published data above [63] room temperature and below [58] room temperature that are not adopted in this phase diagram.

3 Crystal structures at high pressure

Table 1 and Fig. 2 summarize the selected crystallographic information for all the structurally distinct phases of ammonia borane and corresponding references. Detail discussions about these structures are given in the following sections.

3.1 Phase I

At ambient conditions, ammonia borane (Phase I) adopts body-centered tetragonal structure with a space group *I*4*mm*. Lippert et al. [71] and Hughes [72] determined the crystal structure using XRD. However, they were not able to determine the hydrogen atom positions in the structure. Sorokin et al. [78] claimed in 1963 a face-centered orthorhombic structure for this phase, but all later studies confirmed the tetragonal structure [62, 63, 76, 79–81]. The full atomic positions in the *I*4*mm* unit cell were determined by single crystal XRD [76] and neutron diffraction [62, 80, 81]. All these studies consistently indicated that the unit cell consists of two ammonia borane molecules with the B–N bonds parallel to *c*-axis and the hydrogen atoms were disordered in the structure. However, there were discrepancies in the possibilities of the specific locations of these atoms. Bowden et al. [76] conducted single crystal XRD study and showed that the hydrogen atoms occupy positions on mirror planes, 8*c* and 8*d*, with an occupancy of 3/8 to maintain the required stoichiometry. Each of the boron and nitrogen atoms is surrounded by 8 such positions shared by 3 hydrogen atoms. A neutron diffraction study by Yang et al. [81] confirmed this atomic arrangement. However, Hess et al. [80] in their neutron diffraction and molecular simulation study proposed that the disordered hydrogen atoms likely occupy 12 sites around each of the boron and nitrogen atoms on the special position 8*d* and general position 16*e* with an occupancy of 1/4. A later neutron diffraction study by Kumar et al. [62] was favorable to the structure with the 8-site model. NMR studies [73, 82] demonstrated that a high-order rotation about the B–N bond was required for hydrogen atoms presenting possibilities for 12-site model. Nevertheless, a quasi-elastic neutron scattering indicated that 12-fold or higher rotation in the structure was impossible [83]. More experimental and theoretical work is needed to reconcile this discrepancy. The bulk modulus of phase I was determined consistently to be 9.5 GPa by XRD studies [61, 63].

3.2 Phase II

The structure of the low-temperature phase II was first determined experimentally by Hoon and Reynhardt [79] using XRD to be an orthorhombic structure with a space group $Pmn2_1$ and two molecules in the unit cell. Both boron and nitrogen atoms are located on 2*a* positions with B–N bonds parallel to *c*-axis. The locations of the hydrogen atoms were determined with the assistance of their NMR study [73] to be two atoms on each of 2*a* and 4*b* positions, indicating the hydrogen atoms become ordered in this structure. A later neutron diffraction study by Klooster et al. [77] reallocated the boron and nitrogen atoms in the unit cell such that the B–N bonds were no longer parallel to *c*-axis. This structure model was confirmed by the further neutron diffraction study [80].

3.3 Phase III and III′

The pressure-induced phase I to III transition at about 1 GPa was also a disorder-order transition. The structure of phase III was determined to be orthorhombic with a space group of $Cmc2_1$ and 4 molecules in the unit cell by XRD experiments [61, 63]. Assisted with the DFT modeling, the positions of atoms in the unit cell were determined for B and N on the mirror plane 4*a*, and hydrogen at 4*a* and 8*b* positions [61]. This orthorhombic structure was confirmed by a later neutron diffraction study [62]. Across the I–III phase transition, there is about 7 % volume collapse [62, 63].

Table 1 Crystallographic information of ammonia borane phases

Phase	Space group	Z	Unit cell			Atomic positions						Exp. info	Ref.
						B	N	H1	H2	H3	H4		
I	$I4mm$	2	a (Å)	5.2630	x	0	0	0	0	–	–	XRD at 298 K	[76]
			b (Å)	5.2630	y	0	0	0.1480	0.1990	–	–		
			c (Å)	5.0504	z	0.0032	0.6869	0.6190	0.0770	–	–		
II	$Pnm2_1$	2	a (Å)	5.395	x	0	0	0	0.1400	0	0.1850	ND at 200 K	[77]
			b (Å)	4.887	y	0.1850	0.2350	0.4530	0.1480	–0.0430	0.2640		
			c (Å)	4.986	z	0	0.3140	0.3140	0.3970	–0.0600	–0.1000		
III (III′)	$Cmc2_1$	4	a (Å)	5.9958	x	0	0	0	0.1655	0	0.1391	XRD at 1.7 GPa	[61]
			b (Å)	6.4301	y	0.1529	0.2911	0.2689	0.0439	0.1908	0.3839		
			c (Å)	6.0293	z	0.7099	0.9176	0.5519	0.7097	0.0516	0.9350		
IV (IV′)	$P2_1$	4	a (Å)	7.713	$x1$	0.1429	0	−0.0710	0.0826	0.2660	0.4177	XRD, DFT at 15 GPa	[64]
					$x2$	0.3474	0.2724	0.0116	0.2273	0.3539	0.4446		
					$x3$	–	–	−0.0510	0.2261	0.1498	0.2378		
			b (Å)	5.375	$y1$	0.1254	0.6999	0.0549	0.2947	0.7068	0.4449		
					$y2$	0.4594	–	−0.1870	0.1627	0.8397	0.4536		
					$y3$	–	–	0.0334	0.0218	0.7247	0.3028		
			c (Å)	3.898	$z1$	0.1178	0	0.1472	0.2031	0.8816	0.8892		
					$z2$	0.6318	0.6509	0.0374	−0.1100	0.5971	0.4185		
			β (°)	97.22	$z3$	–	–	−0.2390	0.3456	0.5228	0.5827		
V	$Pnma$	4	a (Å)	7.207	$x1$	0.0408	0.1754	−0.1160	0.3123	0.1660	0.1395	XRD, DFT at 6.1 GPa 423 K	[65]
					$x2$	0	0	−0.0720	−0.1540	0	0		
			b (Å)	5.9661	$y1$	0.2500	0.2500	0.2500	0.2500	0.0423	0.4076		
					$y2$	0.1542	0.3102	−0.4160	−0.1120	0.2615	0.2240		
			c (Å)	4.527	$z1$	0.3267	−0.3950	0.4180	−0.4540	−0.2900	−0.0650		
					$z2$	−0.3030	−0.0690	−0.1830	0.2654	−0.4910	0.0941		
VI	$P2_1$	4	a (Å)	5.4766	$x1$	0.2208	0.2874	0.4494	0.1040	0.4616	0.1049	Ab initio MD at 50 GPa	[67]
					$x2$	0.2137	0.2866	0.1500	0.4002	0.2698	0.0847		
					$x3$	–	–	0.2794	0.0975	0.1813	0.3932		
			b (Å)	3.9452	$y1$	0.0803	0.3822	0.3795	0.1665	0.8723	0.6585		
					$y2$	0.5857	0.8890	0.4150	0.9471	0.1046	0.4181		
					$y3$	–	–	0.5973	0.9021	0.9144	0.4381		
			c (Å)	5.4602	$z1$	0.1222	0.9796	0.9186	0.2585	0.7285	0.2764		
			β (°)	103.78	$z2$	0.4757	0.6436	0.8186	0.2405	0.5475	0.5603		
					$z3$	–	–	0.0812	0.9791	0.7667	0.4771		

In their XRD study, Chen et al. [63] first realized that there was no structural change across the III–III′ transition observed in Raman spectroscopy measurement at 5 GPa [55]. However, they were able to detect a change in compressibility, whereas the volume keeps continuous across the transition, and therefore, they concluded that the III–III′ transition was a second-order phase transformation. The bulk moduli for phase III and III′ were reported to be 11.9 and 37 GPa, respectively, with the pressure derivative of modulus $K' = 4.6$. Later XRD and theoretical studies [62, 64] confirmed the identical structure between phase III and III′. Lin et al. [64] also observed the compressibility change across the phase transition with $K = 8.0$ and 12.8 GPa for phase III and III′, respectively, at $K' = 6.4$. The smaller values of the bulk moduli reported by Lin et al. [64] may partially due to the higher K' value they used with regard to those in Chen et al.'s [63] study.

3.4 Phase IV and IV′

The crystal structure for phase IV and IV′ is still under debate. Kumar et al. [62] in 2010 first claimed that above 8 GPa, ammonia borane takes a triclinic structure with the space group of $P1$ and 16 molecules in the unit cell through their DFT calculation and XRD study. Wang et al. [67] in 2011 predicted that phase IV may take a monoclinic structure with $P2_1$ space group in their ab initio molecular dynamics (MD) calculation. The $P2_1$ structure contains 2 molecules in the unit cell. They also predicted that at pressures higher than 25 GPa, another $P2_1$ structure with 4

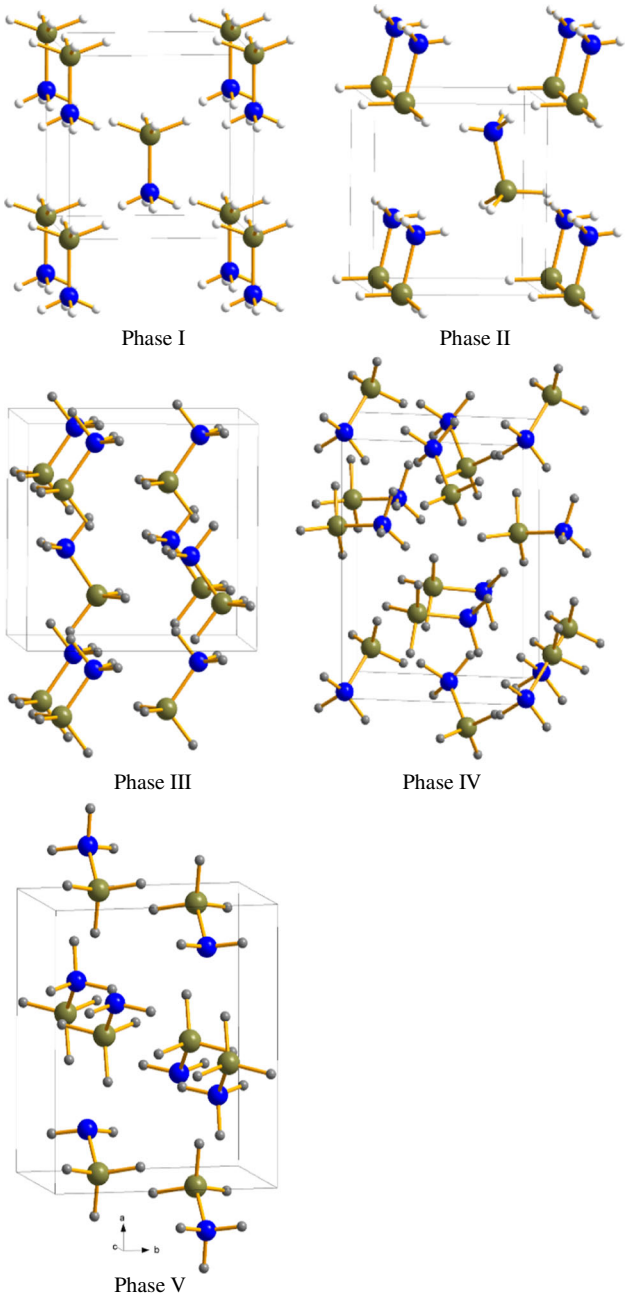

Fig. 2 Crystal structures of different phases of ammonia borane determined through XRD or ND. Large yellow spheres represent boron atoms, large blue spheres represent nitrogen atoms, and small yellow spheres represent hydrogen atoms. Only three equivalent hydrogen atoms are shown in the phase I disordered structure. Phase VI is not included as it has been experimentally confirmed

molecules in the unit cell becomes stable. The more recent XRD and DFT study by Lin et al. [64] in 2012 indicated that the structure of phase IV might actually take a monoclinic structure with the space group of $P2_1$ and 4 molecules in the unit cell. But this monoclinic structure is different from those predicted by Wang et al. [67] although they all take the $P2_1$ space group. All these studies indicated that phase IV to IV′ is an iso-structural transition. Filinchuk et al. [61] in 2009 also pointed out through their ab initio DFT calculation that a $P2_1$ structure might be stable at *P–T* condition between the $Pmn2_1$ and the $Cmc2_1$ structure. But they did not give any details of this structure.

3.5 Phase V

Nylén et al. [65] conducted XRD study at about 6 GPa and high temperatures up to 150 °C. They determined the crystal structure of phase V based on their diffraction data at 6.1 GPa and 150 °C. The structure takes an orthorhombic symmetry with space group of *Pmna* and 4 molecules in the unit cell. The boron and nitrogen atoms are located in 4*c* positions and hydrogen atoms in 4*c* and 8*d* positions.

3.6 Phase VI

According to the theoretical study by Wang et al. [67], phase VI took the $P2_1$ structure with 4 molecules in the unit cell at pressures above 25 GPa. This structure is different from the $P2_1$ structure of phase IV. But so far, this structure has not yet been confirmed by any experimental study.

4 Conclusions

Influence of pressure on ammonia borane has been extensively studied in the past decade. Phase transformations in ammonia borane have been investigated up to 65 GPa at ambient temperature. A brief *P–T* phase diagram is constructed in this paper based on the available experimental and theoretical studies. However, knowledge about the behavior of ammonia borane was still far from comprehensive. Little was known about the phase boundaries at elevated temperatures. Results on the structure of phase IV are controversial. Theoretical and experimental diffraction studies are needed to clarify the low-temperature and high-pressure phase transitions and to solve these low-temperature phases.

Acknowledgments This work was supported by the US Department of Energy, Office of Science, Office of Basic Energy Sciences (DE-FG02-07ER46461). Jiuhua Chen acknowledges part of student support from EFree, an Energy Frontier Research Center funded by DOE-BES (DE-SC000105).

References

1. Shore SG, Parry RW (1955) The crystalline compound ammonia-borane,1 H_3NBH_3. J Am Chem Soc 77:6084–6085
2. Baitalow F, Baumann J, Wolf G et al (2002) Thermal decomposition of B–N–H compounds investigated by using combined thermoanalytical methods. Thermochim Acta 391:159–168

3. T-Raissi A (2002) Hydrogen from ammonia and ammonia-borane complex for fuel cell applications. In: Proceedings of the US DOE Hydrogen Program Review. US Department of Energy, Washington, DC. http://www.eere.energy.gov/hydrogenandfuelcells/annual_review2002.html
4. Langmi HW, McGrady GS (2007) Non-hydride systems of the main group elements as hydrogen storage materials. Coord Chem Rev 251:925–935
5. Chen P, Zhu M (2008) Recent progress in hydrogen storage. Mater Today 11:36–43
6. Umegaki T, Yan JM, Zhang XB et al (2009) Boron- and nitrogen-based chemical hydrogen storage materials. Int J Hydrog Energy 34:2303–2311
7. Smythe NC, Gordon JC (2010) Ammonia borane as a hydrogen carrier: dehydrogenation and regeneration. Eur J Inorg Chem 2010:509–521
8. Staubitz A, Robertson APM, Manners I (2010) Ammonia-borane and related compounds as dihydrogen sources. Chem Rev 110:4079–4124
9. Lan R, Irvine JTS, Tao S (2011) Ammonia and related chemicals as potential indirect hydrogen storage materials. Int J Hydrog Energy 37:1482–1494
10. Wahab M, Zhao H, Yao X (2012) Nano-confined ammonia borane for chemical hydrogen storage. Front Chem Sci Eng 6:27–33
11. Wang P (2012) Solid-state thermolysis of ammonia borane and related materials for high-capacity hydrogen storage. Dalton Trans 41:4296–4302
12. Cecere D, Ingenito A, Giacomazzi E et al (2011) Hydrogen/air supersonic combustion for future hypersonic vehicles. Int J Hydrog Energy 36:11969–11984
13. DOE Fuel Cell Technologies Office (2012) Multi-year research, development, and demonstration plan. http://www1.eere.energy.gov/hydrogenandfuelcells/mypp/
14. Baumann J, Baitalow F, Wolf G (2005) Thermal decomposition of polymeric aminoborane $(H_2BNH_2)_x$ under hydrogen release. Thermochim Acta 430:9–14
15. Hamilton CW, Baker RT, Staubitz A et al (2009) B–N compounds for chemical hydrogen storage. Chem Soc Rev 38:279–293
16. Heldebrant DJ, Karkamkar A, Linehan JC et al (2008) Synthesis of ammonia borane for hydrogen storage applications. Energy Environ Sci 1:156–160
17. Karkamkar AJ, Aardahl CL, Autrey T (2007) Recent developments on hydrogen release from ammonia borane. Mater Matters 2:6–9
18. Stephens FH, Pons V, Baker RT (2007) Ammonia-borane: the hydrogen source par excellence? Dalton Trans 2007:2613–2626
19. Wolf G, Baumann J, Baitalow F et al (2000) Calorimetric process monitoring of thermal decomposition of B–N–H compounds. Thermochim Acta 343:19–25
20. Wolf G, Van Miltenburg J, Wolf U (1998) Thermochemical investigations on borazane $(BH_3–NH_3)$ in the temperature range from 10 to 289 K. Thermochim Acta 317:111–116
21. Stowe AC, Shaw WJ, Linehan JC et al (2007) In situ solid state 11B MAS-NMR studies of the thermal decomposition of ammonia borane: mechanistic studies of the hydrogen release pathways from a solid state hydrogen storage material. Phys Chem Chem Phys 9:1831–1836
22. Shaw WJ, Linehan JC, Szymczak NK et al (2008) In situ multinuclear NMR spectroscopic studies of the thermal decomposition of ammonia borane in solution. Angew Chem Int Ed 47:7493–7496
23. Shevlin SA, Kerkeni B, Guo ZX (2011) Dehydrogenation mechanisms and thermodynamics of MNH_2BH_3 (M = Li, Na) metal amidoboranes as predicted from first principles. Phys Chem Chem Phys 13:7649–7659
24. Jaska CA, Temple K, Lough AJ et al (2001) Rhodium-catalyzed formation of boron–nitrogen bonds: a mild route to cyclic aminoboranes and borazines. Chem Commun 2001:962–963
25. Denney MC, Pons V, Hebden TJ et al (2006) Efficient catalysis of ammonia borane dehydrogenation. J Am Chem Soc 128:12048–12049
26. Paul A, Musgrave CB (2007) Catalyzed dehydrogenation of ammonia-borane by iridium dihydrogen pincer complex differs from ethane dehydrogenation. Angew Chem 119:8301–8304
27. Keaton RJ, Blacquiere JM, Baker RT (2007) Base metal catalyzed dehydrogenation of ammonia-borane for chemical hydrogen storage. J Am Chem Soc 129:1844–1845
28. Yang X, Hall MB (2008) The catalytic dehydrogenation of ammonia-borane involving an unexpected hydrogen transfer to ligated carbene and subsequent carbon–hydrogen activation. J Am Chem Soc 130:1798–1799
29. Zimmerman PM, Paul A, Zhang Z et al (2009) The role of free N-heterocyclic carbene (NHC) in the catalytic dehydrogenation of ammonia-borane in the Nickel NHC system. Angew Chem Int Ed 48:2201–2205
30. Zimmerman PM, Paul A, Musgrave CB (2009) Catalytic dehydrogenation of ammonia borane at ni monocarbene and dicarbene catalysts. Inorg Chem 48:5418–5433
31. Blaquiere N, Diallo-Garcia S, Gorelsky SI et al (2008) Ruthenium-catalyzed dehydrogenation of ammonia boranes. J Am Chem Soc 130:14034–14035
32. Käss M, Friedrich A, Drees M et al (2009) Ruthenium complexes with cooperative PNP ligands: bifunctional catalysts for the dehydrogenation of ammonia-borane. Angew Chem Int Ed 48:905–907
33. Stephens FH, Baker RT, Matus MH et al (2007) Acid initiation of ammonia-borane dehydrogenation for hydrogen storage. Angew Chem Int Ed 46:746–749
34. Alexander J (2010) Dehydrogenation of amine–boranes with a frustrated Lewis pair. Chem Commun 46:1709–1711
35. Guo Y, He X, Li Z et al (2010) Theoretical study on the possibility of using frustrated Lewis pairs as bifunctional metal-free dehydrogenation catalysts of ammonia-borane. Inorg Chem 49:3419–3423
36. Gutowska A, Li L, Shin Y et al (2005) Nanoscaffold mediates hydrogen release and the reactivity of ammonia borane. Angew Chem Int Ed 44:3578–3582
37. Feaver A, Sepehri S, Shamberger P et al (2007) Coherent carbon cryogel-ammonia borane nanocomposites for H_2 storage. J Phys Chem B 111:7469–7472
38. Paolone A, Palumbo O, Rispoli P et al (2009) Absence of the structural phase transition in ammonia borane dispersed in mesoporous silica: evidence of novel thermodynamic properties. J Phys Chem C 113:10319–10321
39. Sepehri S, Feaver A, Shaw WJ et al (2007) Spectroscopic studies of dehydrogenation of ammonia borane in carbon cryogel. J Phys Chem B 111:14285–14289
40. Li Z, Zhu G, Lu G et al (2010) Ammonia borane confined by a metal-organic framework for chemical hydrogen storage: enhancing kinetics and eliminating ammonia. J Am Chem Soc 132:1490–1491
41. Zhao J, Shi J, Zhang X et al (2010) A soft hydrogen storage material: poly(methyl acrylate)-confined ammonia borane with controllable dehydrogenation. Adv Mater 22:394–397
42. Gadipelli S, Ford J, Zhou W et al (2011) Nanoconfinement and catalytic dehydrogenation of ammonia borane by magnesium-metal-organic-framework-74. Chem Eur J 17:6043–6047
43. Fetz M, Gerber R, Blacque O et al (2011) Hydrolysis of ammonia borane catalyzed by aminophosphine-stabilized precursors of

rhodium nanoparticles: ligand effects and solvent-controlled product formation. Chem Eur J 17:4732–4736
44. Wang L-Q, Karkamkar A, Autrey T et al (2009) Hyperpolarized 129Xe NMR investigation of ammonia borane in mesoporous silica. J Phys Chem C 113:6485–6490
45. Kim H, Karkamkar A, Autrey T et al (2009) Determination of structure and phase transition of light element nanocomposites in mesoporous silica: case study of NH_3BH_3 in MCM-41. J Am Chem Soc 131:13749–13755
46. Hélary J, Salandre N, Saillard J et al (2009) A physico-chemical study of an NH_3BH_3-based reactive composition for hydrogen generation. Int J Hydrog Energy 34:169–173
47. Heldebrant DJ, Karkamkar A, Hess NJ et al (2008) The effects of chemical additives on the induction phase in solid-state thermal decomposition of ammonia borane. Chem Mater 20:5332–5336
48. Kalidindi SB, Joseph J, Jagirdar BR (2009) Cu^{2+}-induced room temperature hydrogen release from ammonia borane. Energy Environ Sci 2:1274–1276
49. Xiong Z, Chua Y, Wu G et al (2010) Interaction of ammonia borane with Li_2NH and Li_3N. Dalton Trans 39:720–722
50. Graham K, Kemmitt T, Bowden M (2009) High capacity hydrogen storage in a hybrid ammonia borane–lithium amide material. Energy Environ Sci 2:706–710
51. Bluhm ME, Bradley MG, Butterick R et al (2006) Amineborane-based chemical hydrogen storage: enhanced ammonia borane dehydrogenation in ionic liquids. J Am Chem Soc 128:7748–7749
52. Xiong Z, Yong CK, Wu G et al (2008) High-capacity hydrogen storage in lithium and sodium amidoboranes. Nat Mater 7:138–141
53. Custelcean R, Dreger ZA (2003) Dihydrogen bonding under high pressure: a Raman study of BH_3NH_3 molecular crystal. J Phys Chem B 107:9231–9235
54. Trudel S, Gilson DFR (2003) High-pressure Raman spectroscopic study of the ammonia–borane complex. Evidence for the dihydrogen bond. Inorg Chem 42:2814–2816
55. Lin Y, Mao WL, Drozd V et al (2008) Raman spectroscopy study of ammonia borane at high pressure. J Chem Phys 129:234509
56. Nylén J, Sato T, Soignard E et al (2009) Thermal decomposition of ammonia borane at high pressures. J Chem Phys 131:104506
57. Xie S, Song Y, Liu Z (2009) In situ high-pressure study of ammonia borane by Raman and IR spectroscopy. Can J Chem 87:1235–1247
58. Liu A, Song Y (2011) In situ high-pressure and low-temperature study of ammonia borane by Raman spectroscopy. J Phys Chem C 116:2123–2131
59. Andersson O, Filinchuk Y, Dmitriev V et al (2011) Phase coexistence and hysteresis effects in the pressure–temperature phase diagram of NH_3BH_3. Phys Rev B 84:024115
60. Najiba S, Chen J, Drozd V et al (2013) Ammonia borane at low temperature down to 90 K and high pressure up to 15 GPa. Int J Hydrog Energy 38:4628–4635
61. Filinchuk Y, Nevidomskyy AH, Chernyshov D et al (2009) High-pressure phase and transition phenomena in ammonia borane NH_3BH_3 from X-ray diffraction, Landau theory, and ab initio calculations. Phys Rev B 79:214111
62. Kumar RS, Ke XZ, Zhang JZ et al (2010) Pressure induced structural changes in the potential hydrogen storage compound ammonia borane: a combined X-ray, neutron and theoretical investigation. Chem Phys Lett 495:203–207
63. Chen J, Couvy H, Liu H et al (2010) In situ X-ray study of ammonia borane at high pressures. Int J Hydrog Energy 35:11064–11070
64. Lin Y, Ma H, Matthews CW et al (2012) Experimental and theoretical studies on a high pressure monoclinic phase of ammonia borane. J Phys Chem C 116:2172–2178
65. Nylén J, Eriksson L, Benson D et al (2013) Characterization of a high pressure, high temperature modification of ammonia borane (BH_3NH_3). J Chem Phys 139:054507
66. Baitalow F, Wolf G, Grolier JPE et al (2006) Thermal decomposition of ammonia-borane under pressures up to 600 bar. Thermochim Acta 445:121–125
67. Wang L, Bao K, Meng X et al (2011) Structural and dynamical properties of solid ammonia borane under high pressure. J Chem Phys 134:024517
68. Ramzan M, Ahuja R (2010) High pressure and temperature study of hydrogen storage material BH_3NH_3 from ab initio calculations. J Phys Chem Solids 71:1137–1139
69. Sun Y, Chen J, Drozd V et al (2014) Phase boundary of pressure-induced *I*4*mm* to *Cmc*21 transition in ammonia borane at elevated temperature determined using Raman spectroscopy. Int J Hydrog Energy 39:8293–8302
70. Kupenko I, Dubrovinsky L, Dmitriev V et al (2012) In situ Raman spectroscopic study of the pressure induced structural changes in ammonia borane. J Chem Phys 137:074506
71. Lippert EL, Lipscomb WN (1956) The structure of H_3NBH_3. J Am Chem Soc 78:503–504
72. Hughes EW (1956) The crystal structure of ammonia-borane, H_3NBH_3. J Am Chem Soc 78:502–503
73. Reynhardt EC, Hoon CF (1983) Molecular dynamics and structures of amine boranes of the type $R_3N{\cdot}BH_3$. II. NMR investigation of $H_3N{\cdot}BH_3$. J Phys C Solid State Phys 16:6137–6152
74. Hess NJ, Bowden ME, Parvanov VM et al (2008) Spectroscopic studies of the phase transition in ammonia borane: Raman spectroscopy of single crystal NH_3BH_3 as a function of temperature from 88 to 330 K. J Chem Phys 128:034508
75. Najiba S, Chen J, Drozd V et al (2012) Tetragonal to orthorhombic phase transition of ammonia borane at low temperature and high pressure. J Appl Phys 111:112618
76. Bowden ME, Gainsford GJ, Robinson WT (2007) Room-temperature structure of ammonia borane. Aust J Chem 60:149–153
77. Klooster WT, Koetzle TF, Siegbahn PEM et al (1999) Study of the N−H···H−B dihydrogen bond including the crystal structure of BH_3NH_3 by neutron diffraction. J Am Chem Soc 121: 6337–6343
78. Sorokin VP, Vesnina BI, Klimova NS (1963) Ammonia-borane: a new method of preparation, and its properties. Zhurnal Neorganicheskoi Khimii 8:66–68
79. Hoon CF, Reynhardt EC (1983) Molecular dynamics and structures of amine boranes of the type $R_3N{\cdot}BH_3$. I. X-ray investigation of $H_3N{\cdot}BH_3$ at 295 and 110 K. J Phys C Solid State Phys 16:6129–6136
80. Hess NJ, Schenter GK, Hartman MR et al (2009) Neutron powder diffraction and molecular simulation study of the structural evolution of ammonia borane from 15 to 340 K. J Phys Chem A 113:5723–5735
81. Yang JB, Lamsal J, Cai Q et al (2008) Structural evolution of ammonia borane for hydrogen storage. Appl Phys Lett 92:091916
82. Penner GH, Chang YCP, Hutzal J (1999) A Deuterium NMR spectroscopic study of solid BH_3NH_3. Inorg Chem 38:2868–2873
83. Brown CM, Jacques TL, Hess NJ et al (2006) Dynamics of ammonia borane using neutron scattering. Phys B Condens Matter 385–386:266–268